

Plasma astrophysics in numerical simulations



A. Nordlund

Simulations of astrophysical dynamos

Axel Brandenburg

NORDITA, AlbaNova University Center, Roslagstullsbacken 23, SE-10691 Stockholm, Sweden;
Department of Astronomy, Stockholm University, SE 10691 Stockholm, Sweden

Abstract. Numerical aspects of dynamos in periodic domains are discussed. Modifications of the solutions by numerically motivated alterations of the equations are being reviewed using the examples of magnetic hyperdiffusion and artificial diffusion when advancing the magnetic field in its Euler potential representation. The importance of using integral kernel formulations in mean-field dynamo theory is emphasized in cases where the dynamo growth rate becomes comparable with the inverse turnover time. Finally, the significance of microscopic magnetic Prandtl number in controlling the conversion from kinetic to magnetic energy is highlighted.

Keywords. Sun: magnetic fields

1. Introduction

There are two important aspects connected with astrophysical dynamos compared with dynamos on a bicycle. Firstly, they are self-excited and do not require any permanent magnets. Secondly, they are *homogeneous* in the sense that the medium is conducting everywhere in the dynamo proper and there are no wires or insulators inside. Self-excited dynamos were invented by the Danish inventor Søren Hjørrth, who received the patent for this discovery in 1854, some 12 years before Samuel Alfred Varley, Ernst Werner von Siemens and Charles Wheatstone announced such an invention independently of each other. Von Siemens is known for having recognized its industrial importance in producing the most powerful generators at the time, for which he, in turn, received a patent in 1877.

The idea that homogeneous dynamos might work in the Sun, was first proposed by Larmor (1919) in a one-page paper. However, some 14 years later, Cowling (1933) showed that axisymmetric dynamos cannot work in a body like the Sun. At the time it was not clear whether this failure was genuine, or whether it was critically connected with Cowling's assumption of axisymmetry. The suspicion that the third dimension might be critical was not particularly emphasized when Larmor (1934) tried to defend his early suggestion with the words "the self-exciting dynamo analogy is still, so far as I know, the only foundation on which a gaseous body such as the Sun could possess a magnetic field: so that if it is demolished there could be no explanation of the Sun's magnetic field even remotely in sight."

The essential idea about the operation of the solar dynamo came from Parker (1955), who developed the notion that cyclonic events would tilt a toroidal field systematically in the poloidal direction, closing thereby a critical step in the dynamo cycle. While this concept is still valid today, it still required the existence proof by Herzenberg (1958) that began to convince critics that Cowling's antidynamo theorem does not extend to the general case of three dimensions.

Nevertheless, subsequent progress in modeling the solar dynamo appears to have been suspended until the foundations of a mean-field treatment of the induction equation were developed by Steenbeck *et al.*, (1966). In the following years, a large number of models were computed covering mostly aspects of the solar dynamo (Steenbeck & Krause, 1969a; Parker, 1970a; Parker, 1970b; Parker, 1970c; Parker, 1971b; Parker, 1971d; Parker,

1971f), but in some cases also terrestrial dynamos (Steenbeck & Krause, 1969b; Parker, 1971c) and the galactic dynamo (Parker, 1971a; Parker, 1971e; Vainshtein & Ruzmaikin, 1971; Vainshtein & Ruzmaikin, 1972). These developments provided a major boost to dynamo theory given that until then work on the galactic dynamo, for example, focussed on aspects concerning the small-scale magnetic field (Parker, 1969), but not the global large-scale fields on the scale of the entire galaxy. In fact, also regarding small-scale dynamos, there were important developments made by Kazantsev (1968), but they remained mostly unnoticed in the West, even when the first direct simulations by Meneguzzi *et al.* (1981) demonstrated the operation of such a dynamo in some detail. In fact, in some of these dynamos, the driving of the flow involved helicity, but its role in helping the dynamo remained unconvincing, because no large-scale field was produced. We now understand that this was mainly because there was not enough scale separation between the scale of the domain and the forcing scale, and that one needs at least a ratio of 3 (Haugen *et al.*, 2004).

Simulations in spherical geometry were much more readily able to demonstrate the production of large-scale magnetic fields (Gilman, 1983; Glatzmaier, 1985), but even today these simulations produce magnetic fields that propagate toward the poles (Käpylä *et al.*, 2010) and not toward the equator, as in the Sun. We can only speculate about possible shortcomings of efforts such as these that must ultimately be able to reproduce the solar cycle.

Several important developments happened in the 1980s. Firstly, it became broadly accepted that the magnetic field inside the Sun might be in a fibril state (Parker, 1982), i.e. the filling factor is small and most of the field is concentrated into thin flux tubes, as manifested by the magnetic field appearance in the form of sunspots at the surface. However, such tubes would be magnetically buoyant, and are expected to rise to the surface on a time scale of some 50 days (Moreno-Insertis, 1983; Moreno-Insertis, 1986). This time is short compared with the cycle time and might lead to excessive magnetic flux losses, which then led to the proposal that the magnetic field would instead be generated in the overshoot layer beneath the convection zone. This idea is still the basic picture today, although simulations of convection generally produce magnetic fields that are distributed over the entire convection zone.

Yet another important development in the 1980s was the proposal that the α effect might actually be the sum of a kinetic and a magnetic part and that the magnetic part can be estimated by solving an evolution equation for the magnetic helicity density. The importance of this development was obscured by the excitement that the two evolution equations for poloidal and toroidal field, supplemented by a third equation for the magnetic helicity density, could produce chaos (Ruzmaikin, 1981). The connection to what was to come some 10–20 years later was not yet understood at that point. Simulations of helical MHD turbulence in a periodic domain demonstrated that in a periodic domain the α effect might be quenched in an Re_M -dependent fashion like

$$\alpha = \frac{\alpha_0}{1 + Re_M \overline{\mathbf{B}}^2 / B_{eq}^2}. \tag{1.1}$$

If this were also true of astrophysical dynamos, α would be negligibly small and would not be relevant for explaining the magnetic field in these bodies. Such quenching is therefore nowadays referred to as catastrophic quenching. However, there is now mounting evidence that this type of α quenching is a special case of a more general formula (Brandenburg, 2008)

$$\alpha = \frac{\alpha_0 + Re_M [\eta_t \mu_0 \overline{\mathbf{J}} \cdot \overline{\mathbf{B}} / B_{eq}^2 - (\nabla \cdot \overline{\mathbf{F}}_C) / 2k_f^2 B_{eq}^2 - (\partial\alpha/\partial t) / 2\eta_t k_f^2]}{1 + Re_M \overline{\mathbf{B}}^2 / B_{eq}^2}, \tag{1.2}$$

which comes from magnetic helicity conservation. Note that in this equation there are 3 new terms that all scale with Re_M and are therefore important. Even in a closed or periodic domain, the first and third terms in squared brackets contribute, the most promising way out of catastrophic quenching is through magnetic helicity fluxes (Blackman & Field, 2000; Kleorin *et al.*, 2000). These developments are still ongoing and we refer here to some recent papers by (Shukurov *et al.*, 2006; Brandenburg *et al.*, 2009; Candelaresi *et al.*, 2010).

2. Simulating dynamos

2.1. Roberts flow

Much of the theoretical understanding of dynamos is being helped by numerical simulations. In fact, nowadays one of the simplest dynamos to simulate is the Roberts flow dynamo. A kinematic dynamo can be simulated by adopting a velocity field of the form

$$\mathbf{U} = \nabla \times \psi \mathbf{z} + k_f \psi \mathbf{z}, \quad (2.1)$$

where $\psi = (U_0/k_0) \cos k_0 x \cos k_0 y$. In order to give some idea about the ease at which reasonably accurate solutions can be obtained we give in Table 1 the numerically obtained critical values of the magnetic Reynolds number, $\text{Re}_M = u_{\text{rms}}/\eta k_f$, for a given resolution.

Table 1. Critical values of Re_M for the Roberts flow dynamo at low resolution (from 8^3 to 32^3 mesh points) and different spatial order of the numerical scheme.

Resolution	— $\text{Re}_M c$ —		
	2nd order	6th order	8th order
8^3	5.23	5.15	5.16
16^3	5.517	5.514	5.518
32^3	5.522	5.522	5.521

Even turbulent dynamos are nowadays easy to simulate and meaningful results have been obtained already at relatively low resolution, provided the flow is helical (Brandenburg, 2001). However, there are also examples where numerical aspects can have a major effect on the outcome of such simulations. In the following we discuss two examples: magnetic hyperdiffusion and the use of Euler potential with artificial magnetic diffusion.

2.2. Magnetic hyperdiffusion in helicity-driven dynamos

Dynamos work by maintaining the magnetic field against Ohmic decay via magnetic induction. It is then not surprising that the result can be sensitive to the numerical treatment of magnetic diffusion. One example is the consideration of magnetic hyperdiffusion of the form

$$\eta \mathbf{J} \rightarrow (-1)^{n-1} \nu_n \nabla^2 a^{2n-2} \mathbf{J} \quad (2.2)$$

instead of the regular $\eta \mathbf{J}$ term. In helical dynamos in closed or periodic domains the saturation time is given by $\eta k_1^2 \Delta t = 1$, but with hyperdiffusion this condition becomes $\eta_n k_1^{2n} \Delta t = 1$; see Figure 1. This is exactly what one expects from a scheme like hyperdiffusion that enhances the effective magnetic Reynolds number. However, another important modification is that the saturation amplitude increases from Brandenburg & Sarson, 2002

$$\frac{\overline{\mathbf{B}}^2}{B_{\text{eq}}^2} \approx \frac{k_f}{k_1} \quad \text{to} \quad \frac{\overline{\mathbf{B}}^2}{B_{\text{eq}}^2} \approx \left(\frac{k_f}{k_1} \right)^{2n-1}. \quad (2.3)$$

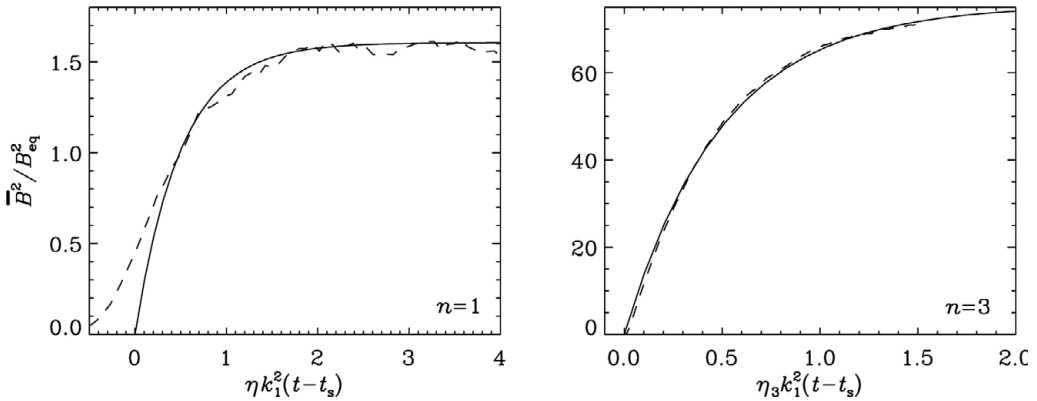


Figure 1. Evolution of large-scale magnetic field (dashed lines) for runs with regular magnetic diffusion ($n = 1$, left, $u_{\text{rms}}/\eta k_1 = 45$) and magnetic hyperdiffusion ($n = 3$, right, $u_{\text{rms}}/\eta_3 k_1 = 3200$), at 16^3 resolution and $k_f/k_1 = 3$, compared with the prediction (solid lines) of Brandenburg & Sarson, 2002, where t_s is the saturation time of the small-scale field.

This is a caveat that is important to keep in mind when employing magnetic hyperdiffusion for astrophysical simulations. This has a major effect on the saturation of large-scale magnetic fields that is at first glance surprising. However, once one realizes that the saturation in a periodic domain is governed by the magnetic helicity equation applied to the steady state, i.e. by

$$\frac{d}{dt} \langle \mathbf{A} \cdot \mathbf{B} \rangle = -2\eta \langle \mathbf{J} \cdot \mathbf{B} \rangle, \tag{2.4}$$

where we split the right-hand side into contributions from large- and small-scale fields, i.e. $\mathbf{B} = \overline{\mathbf{B}} + \mathbf{b}$ and $\mathbf{J} = \overline{\mathbf{J}} + \mathbf{j}$, so that $\langle \mathbf{J} \cdot \mathbf{B} \rangle = \langle \overline{\mathbf{J}} \cdot \overline{\mathbf{B}} \rangle + \langle \mathbf{j} \cdot \mathbf{b} \rangle$, we have for fully helical large- and small-scale fields in the steady state,

$$0 = -2\eta \langle \overline{\mathbf{J}} \cdot \overline{\mathbf{B}} \rangle - 2\eta \langle \mathbf{j} \cdot \mathbf{b} \rangle \approx \pm 2\eta \left(k_1 \langle \overline{\mathbf{B}}^2 \rangle - k_f \langle \mathbf{b}^2 \rangle \right), \tag{2.5}$$

with $\langle \mathbf{b}^2 \rangle \approx B_{\text{eq}}^2$, it becomes clear that the use of magnetic hyperdiffusion picks up the k_1 and k_f factors at correspondingly higher powers, leading thus to Equation 2.3. The upper and lower signs of the term on the right-hand side of Equation 2.5 apply to small-scale forcings with positive and negative helicity, respectively.

2.3. MHD with Euler potentials

Until recently, the use of Euler potentials (EP) has been a popular choice for solving the MHD equations numerically using Lagrangian methods (Price & Bate, 2007; Rosswog & Price, 2007).

The representation of \mathbf{B} in terms of EP, α and β , as

$$\mathbf{B} = \nabla\alpha \times \nabla\beta \tag{2.6}$$

is a nonlinear one, which solves the induction equation in the case $\eta = 0$, $\partial\mathbf{B}/\partial t = \nabla \times (\mathbf{U} \times \mathbf{B})$, provided $D\alpha/Dt = D\beta/Dt = 0$. The problem is that the magnetic field tends to develop sharp structures that will not be properly resolved by the numerical scheme. The hope has been that the overall properties of the magnetic field at larger scales would then still be approximately correct. However, this turns out not to be the case. And, more importantly, as one increases the resolution, the solution converges, but it is simply the wrong solution. This has been demonstrated in detail in a separate paper

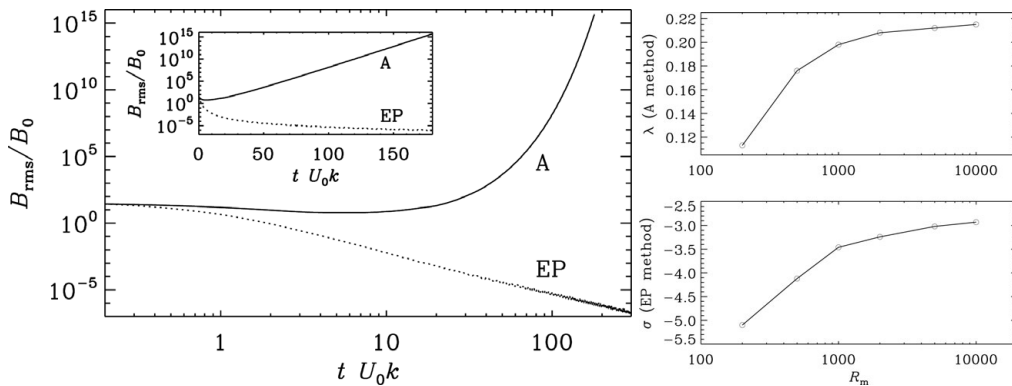


Figure 2. Left: Comparison of the evolution of B_{rms} for the modified Galloway–Proctor flow with point-wise zero helicity for methods A and EP using 256^3 meshpoints and $\text{Re}_M = 10^4$. Note the power law scaling for the EP method and the exponential scaling for the A method. Right: Re_M dependence of the exponents λ and σ characterizing the evolution of $B_{\text{rms}} \sim e^{\lambda t}$ for the A method and $B_{\text{rms}} \sim t^\sigma$ for the EP method for the modified Galloway–Proctor flow with point-wise zero helicity for methods A and EP using 256^3 meshpoints. Adapted from Brandenburg (2010).

(Brandenburg, 2010) where, among other cases, solutions of the Galloway–Proctor fast dynamo flow were considered. In Figure 2 we show that the solution of the induction equation using EP leads to algebraically decaying solutions of the form

$$B_{\text{rms}} \sim t^\sigma \quad (\text{EP method}), \quad (2.7)$$

where, with increasing resolution, σ converges toward a value around -3 , while with the usual vector potential method (A method) one solves $\partial \mathbf{A} / \partial t = \mathbf{U} \times \mathbf{B} - \eta \mathbf{J}$ with $\mathbf{B} = \nabla \times \mathbf{A}$ and $\mathbf{J} = \nabla \times \mathbf{B}$, and finds instead

$$B_{\text{rms}} \sim e^{\lambda t} \quad (\text{A method}), \quad (2.8)$$

where λ also converges, and its value is about 0.22 for $\text{Re}_M = 10^4$; see Figure 2.

It is quite remarkable that by changing the properties of the solution at small scales only slightly, one can produce rather dramatic effects. This includes cases of magnetic hyperdiffusivity, where the large-scale field amplitude can be quite different, albeit in agreement with the theory applied to the hyperdiffusive case (Brandenburg & Sarson, 2002). Another example is that of artificial diffusion in solutions for the EP, where the obtained results bear no resemblance with those obtained using the A method.

2.4. Quantitative comparison between simulations and mean-field theory

Mean-field theory has the potential of being a quantitatively accurate and hence predictive theory. In order to establish this in particular cases, it is important to consider as many contact points between theory and simulations as possible. One thing we can do is to determine α effect, turbulent diffusion, and other effects from simulations, and to compare the thus calibrated mean-field model with simulations. This provides an important resource for ideas of what one might have been missing in various contexts. Here we just mention the case of the Roberts flow, for which α_{ij} and η_{ij} have been determined using the test-field methods (Schrinner *et al.*, 2007). One might then expect that the growth rate obtained from the underlying dissipation rate,

$$\lambda = \alpha k - (\eta_t + \eta) k^2 \quad (2.9)$$

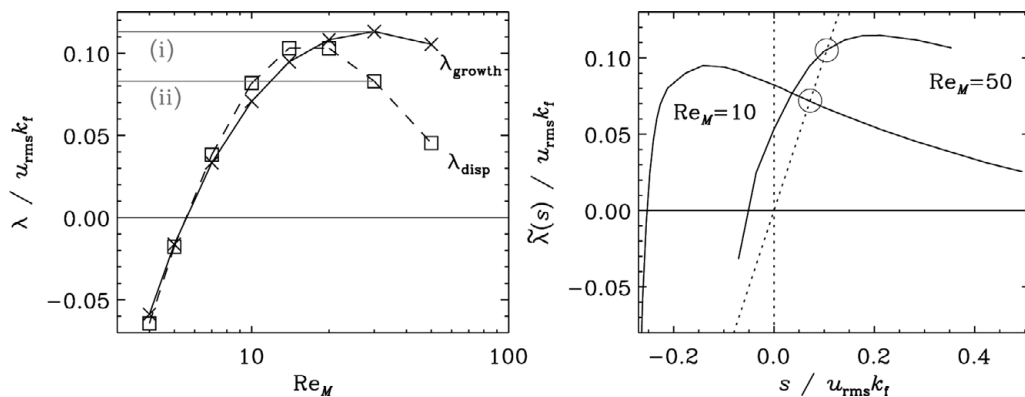


Figure 3. Left: Re_M dependence of the growth rate for the Roberts flow as obtained from a direct calculation (λ_{growth}) compared with the result of the dispersion relation, $\lambda_{\text{disp}} = \alpha k_z - (\eta + \eta_t) k_z^2$, using a cubic domain of size L^3 , where $k_1 = 2\pi/L$ and $k_t = \sqrt{2}k_1$. For this range of Re_M , the most unstable mode is the largest one that fits in the box ($k_z = k_1$). The two horizontal lines in gray mark the values of λ_{growth} and λ_{disp} at $Re_M = 30$, denoted by (i) and (ii), respectively. Right: Laplace-transformed effective growth rate, $\tilde{\lambda}(s) = \tilde{\alpha}(s)k - [\eta + \tilde{\eta}_t(s)]k^2$, for the Roberts flow with $Re_M = 10$ and 50 . Note the different signs of the slope at the intersection with the diagonal (denoted by circles). Adapted from Hubbard & Brandenburg (2009).

should agree with the value obtained from the direct calculation. This is however only the case for $\lambda = 0$, but not for $\lambda \neq 0$. However, it would be a mistake to assume that there is something wrong with the test-field methods. Instead, what is wrong here is just the assumption of homogeneity and stationarity. Obviously, when $\lambda \neq 0$, the solution is exponentially growing or decaying like $e^{\lambda t}$, so it is clearly not steady!

When the assumption of steadiness is no longer satisfied, one has to return to the underlying integral relation between α and the mean field, i.e. $\alpha(z, t)\overline{\mathbf{B}}(z, t)$ has to be replaced by a convolution, so

$$\alpha(z, t)\overline{\mathbf{B}}(z, t) \rightarrow \int \alpha(z - z', t - t')\overline{\mathbf{B}}(z', t') dz' dt', \tag{2.10}$$

and similarly for the magnetic diffusivity. One way of dealing with this complication is to note that the convolution in real space corresponds to a multiplication in Fourier space. In other words, we can write

$$\tilde{\mathcal{E}}(k, \omega) = \tilde{\alpha}(k, \omega)\tilde{\mathbf{B}}(k, \omega), \tag{2.11}$$

where $\tilde{\mathcal{E}}(k, \omega) = \int \overline{\mathcal{E}}(z, t) e^{-i(kz - \omega t)} dz dt$ is the Fourier-transformation of $\overline{\mathcal{E}}(z, t)$ (and likewise for the other fields). Of course, the value of ω that is of interest is $\omega = i\lambda$, where λ is the then self-consistently obtained growth rate. This has been described in detail by Hubbard & Brandenburg (2009), who motivated their study using the example of the Roberts flow, where the discrepancy between the numerical solution and that obtained for $\lambda = 0$ is shown. A reasonable fit to their data is $\alpha(k, \omega) = 1/(1 - i\omega\tau)$ for $k \rightarrow 0$.

3. Low magnetic Prandtl number and application to accretion discs

In many astrophysical bodies the magnetic Prandtl number, $Pr_M = \nu/\eta$, is either large or small, but not around unity. Again, from a numerical point of view, it is surprising that the ratio ν/η is important even though

$$\nu \rightarrow 0, \quad \eta \rightarrow 0. \tag{3.1}$$

In many numerical treatments it is implicitly assumed that the exact values of ν and η do not explicitly matter, because it should not matter how long each of the two turbulent cascades is. This should indeed be true provided the dynamics we are interested in takes place entirely on the large scales. But for helical large-scale dynamos, this is evidently not the case, because in the kinematic regime, the magnetic energy spectrum follows the Kazantsev $k^{3/2}$ spectrum and reaches a peak at the resistive scale, corresponding to the wavenumber $k_\eta = (J_{\text{rms}}/\eta)$. However, this applies first of all only to the kinematic regime and, seemingly, it is relevant only for the small-scale dynamo regime. This has been discussed recently in connection with the contrasting case of large-scale dynamos, where the excitation conditions are not affected by the value of Pr_M (Brandenburg, 2009; Brandenburg, 2011). Nevertheless, even in this case the dissipation rates of kinetic and magnetic energies, ϵ_K and ϵ_M , respectively, do depend on the value of Pr_M . Although it seems fairly clear that the ratio ϵ_K/ϵ_M increases with Pr_M in power law fashion proportional to Pr_M^n , the exponent n is not well constrained. Earlier work covering the range $10^{-3} \leq \text{Pr}_M \leq 1$ at 512^3 resolution suggested $n = 1/2$, although additional data covering also the range $1 < \text{Pr}_M \leq 10^3$ given an exponent closer to $n = 0.6$ or even $n = 2/3$. There is at present no theory for the value of the exponent n .

Applying these findings to accretion discs, we should first recall that the work of Lesur & Longaretti (2007) suggested that the onset of the magneto-rotational instability shows a strong dependence on Pr_M . However, one should expect that when large-scale dynamo action is possible, this condition may change and the onset would then be independent of Pr_M . This is indeed what Käpylä & Korpi (2010) find. The question is of course what is the relevant large-scale dynamo mechanism in this case. One proposal is the incoherent α -shear dynamo, which works through constructive amplification of the mean field in the direction of mean shear. Yet another possible mechanism is the shear-current dynamo (Rogachevskii & Kleeorin, 2003), although this result has not yet been confirmed.

4. Conclusions

Simulating simple dynamos on the computer is nowadays quite simple. Nevertheless, we have seen here examples that illustrate that things can also go quite “wrong”. In the case of magnetic hyperdiffusion, it is clear what happens (Brandenburg & Sarson, 2002), so that magnetic hyperdiffusion can also be used to ones advantage, as was demonstrated in Brandenburg *et al.* (2002). However, in the case of Euler potentials it is not clear what happens and whether this method can be used to simulate even the ideal MHD equations, given that each numerical scheme will introduce some type of diffusion. In this short review, we have also attempted to clarify why numerical calculations of α effect and turbulent diffusion using the standard test-field method (Schrinner *et al.*, 2007) would yield values that can only reproduce a correct growth rate in the case of vanishing growth. In all other case, a representation in terms of integral kernels has to be used. Finally, we have discussed some effects of using magnetic Prandtl numbers that are different from unity. It turns out that in the steady state, the rate of transfer from kinetic to magnetic energy depends on the value of Pr_M . This is somewhat unexpected, because the onset condition for dynamo action does not depend on Pr_M (Brandenburg, 2009), and yet the actual efficiency of the dynamo, as characterized by the work done against the Lorentz force, $-\langle \mathbf{U} \cdot (\mathbf{J} \times \mathbf{B}) \rangle$, does depend on Pr_M and is proportional to Pr_M^{-n} (with n between $1/2$ and $2/3$) for large values of Pr_M .

Understanding the limits of numerical simulations is just as important as appreciating its powers. As the example with the problem with mean-field and simulated growth rates shows, understanding the initial mismatch can be the key to a more advanced and

more accurate theory that will ultimately be needed when describing some of the yet unexplained properties of astrophysical dynamos.

References

- Blackman, E. G. & Field, G. B., *MNRAS* 2000, *318*, 724
 Brandenburg, A., *ApJ*, 2001, *550*, 824
 Brandenburg, A. *Astron. Nachr.*, 2008, *329*, 725
 Brandenburg, A. *ApJ*, 2009, *697*, 1206
 Brandenburg, A. *MNRAS*, 2010, *401*, 347
 Brandenburg, A. *Astron. Nachr.*, 2011, *332*, 51 (arXiv:1008.4226)
 Brandenburg, A. & Sarson, G. R. *Phys. Rev. Lett.*, 2002, *88*, 055003
 Brandenburg, A., Candelaresi, S., & Chatterjee, P. *MNRAS* 2009, *398*, 1414
 Brandenburg, A., Dobler, W., & Subramanian, K. *Astron. Nachr.*, 2002, *323*, 99
 Candelaresi, S., Hubbard, A., Brandenburg, A., & Mitra, D. 2010 (arXiv:1010.6177)
 Cowling, T. G. *MNRAS*, 1933, *94*, 39
 Gilman, P. A. *ApJS*, 1983, *53*, 243
 Glatzmaier, G. A. *ApJ*, 1985, *291*, 300
 Herzenberg, A. *Proc. Roy. Soc. Lond.*, 1958, *250A*, 543
 Haugen, N. E. L., Brandenburg, A., & Dobler, W. *Phys. Rev. E*, 2004, *70*, 016308
 Hubbard, A. & Brandenburg, A. *ApJ*, 2009, *706*, 712
 Käpylä, P. J. & Korpi, M. J. 2010 (arXiv:1004.2417)
 Käpylä, P. J., Korpi, M. J., Brandenburg, A., *et al.* *Astron. Nachr.*, 2010, *331*, 73
 Kazantsev, A. P. *Sov. Phys. JETP*, 1968, *26*, 1031
 Kleorin, N., Moss, D., Rogachevskii, I., & Sokoloff, D. *A&A*, 2000, *361*, L5
 Larmor, J. 1919 *Rep. Brit. Assoc. Adv. Sci.* 159
 Larmor, J. *MNRAS*, 1934, *94*, 469
 Lesur, G. & Longaretti, P.-Y. *A&A*, 2007, *378*, 1471
 Meneguzzi, M., Frisch, U., & Pouquet, A. *Phys. Rev. Lett.*, 1981, *47*, 1060
 Moreno-Insertis, F. *A&A*, 1983, *122*, 241
 Moreno-Insertis, F. *A&A*, 1986, *166*, 291
 Parker, E. N. *ApJ*, 1955, *122*, 293
 Parker, E. N. *ApJ*, 1982, *256*, 302
 Parker, E. N. *ApJ*, 1969, *157*, 1129
 Parker, E. N. *ARA&A*, 1970a, *8*, 1
 Parker, E. N. *ApJ*, 1970b, *160*, 383
 Parker, E. N. *ApJ*, 1970c, *162*, 665
 Parker, E. N. *ApJ*, 1971a, *163*, 255
 Parker, E. N. *ApJ*, 1971b, *163*, 279
 Parker, E. N. *ApJ*, 1971c, *164*, 491
 Parker, E. N. *ApJ*, 1971d *165*, 139
 Parker, E. N. *ApJ*, 1971e *166*, 295
 Parker, E. N. *ApJ*, 1971f *168*, 239
 Price, D. J. & Bate, M. R. *MNRAS*, 2007, *377*, 77
 Rogachevskii, I. & Kleorin, N. *Phys. Rev. E*, 2003, *68*, 036301
 Rosswog, S. & Price, D. *MNRAS*, 2007, *379*, 915
 Ruzmaikin, A. A. 1981 *Comments Astrophys.*, *9* 85
 Schinner, M. Rädler, K.-H., Schmitt, D., *et al.* *Geophys. Astrophys. Fluid Dyn.*, 2007, *101*, 81
 Shukurov, A., Sokoloff, D., Subramanian, K., & Brandenburg, A. *A&A*, 2006, *448*, L33
 Steenbeck, M. & Krause, F. *Astron. Nachr.*, 1969a, *291*, 49
 Steenbeck, M. & Krause, F. *Astron. Nachr.*, 1969b, *291*, 271
 Steenbeck, M., Krause, F., & Rädler, K.-H. 1966, *Z. Naturforsch.*, *21a*, 369
 Vainshtein, S. I. & Ruzmaikin, A. A. 1971, *Astron. Zh.*, *48*, 902
 Vainshtein, S. I. & Ruzmaikin, A. A. 1972, *Astron. Zh.*, *49*, 449